"Analysis of Stress in Block during Rolling by Visioplasticity Method"

By

Natsuo HATTA* and Jun-ichi KOKADO*

(Received June 11, 1979)

Abstract

In this paper, the visioplasticity analysis on stress in block during rolling is discussed, and then the calculable results of the stress concerning the inside and surface of block are presented. This stress analysis depends considerably on the accuracy of the rolling test, which is carried out in order to determine the flow lines. It is very difficult to deduce the validity of the calculable results in detail because of the lack of measured examples on the stress in block.

However, the measured rolling force by a load cell coincides extremely well with the one obtained from the stress in the thickness direction which is calculated here. The neutral point seems to exist on the valid position. Of course, the validity of the calculated results cannot be concluded from only two points. However, it may be possible to apply the visioplasticity method for the calculation of the stress in block, if the exact flow line can be determined.

I. Introduction

In the field of the rolling theory carried out till now, investigations concerning the pressure distribution on the contact surface between the rolls and the material abound. For the theoretical investigations of flat rolling, the first representative rolling analyses were carried out by von Karman[1], Trinks[2], Nadai[3], Orowan[4] and Sims[5] and many others. For the experimental investigations of rolling, Siebel and Lueg[6] made the first actual survey of the pressure distribution on the contact surface between rolls and material by using the piezoelectric effect. Comparatively lately, Matsuura and Motomura[7] measured the pressure distribution by the pin contact method, when the material with a rectangular cross section is rolled in grooved box passes with several wall angles.

However, investigations on the stress distribution of the inner part of the material during rolling have been scarcely carried out. In recent years, Toyo-

* Department of Mineral Science and Technology

shima and Koga[8] tried to measure the horizontal and vertical stress in the plasticin test piece, in which micro pressure sensors were set at four levels in cross section.

In this paper, the visioplasticity analysis on stress in block during rolling is discussed, and then calculated results of the stress concerning the inside and surface of block are presented. This visioplasticity method was originally developed by E.G. Thomsen.[9] Several examples applying this method to the axisymmetric extrusion through a tapered die etc. were already reported.[10)~13)] This visioplasticity method consists of determinting several flow lines by rolling tests, obtaining the velocity field from the flow lines and calculating the complete strain rate, strain and stress by considering the equilibrium and plasticity equations.

In the case of applying this method to flat rolling, the reliability of the calculated values of flow velocity, strain rate, strain and stress are remarkably influenced by the accuracy of flow lines, which are determined by the rolling test. Therefore, the movement of the material in a zigzag direction and the warp of the material in upper and lower directions must be absolutely protected during rolling.

This paper shows a series of the calculated results from the velocity field to the stress by using the flow lines obtained by the rolling test of Al-plate, on the assumption of the plane strain deformation without the spread of the width. At the same time, stress solutions by the visioplasticity method in the case of the three-dimensional deformation are stated.

II. Fundamental theory

2.1 Flow function

Rolling of material as an industrial process consists of passing a billet, sheet or strip between rolls to reduce its thickness. In this case, the flow lines from the start of the deformation to the end are obtained by stopping to drive rolls on the way of the rolling of the plate with some regular patterns on the side plane perpendicular to the width. In the case of flat rolling, the deformation of the rolled material is symmetrical for the center of the thickness. Therefore, for convenience, the x- and z-axis are taken in the direction of center line of the plate thickness and in the direction of thickness, as shown in Fig.1. From the fact that the direction of the tangent which touches the flow line corresponds exactly to that of velocity, the equation of the flow line is as follows:

$$u \cdot dz - v \cdot dx = 0 . \qquad (1)$$

Here, u and v show the velocity components in the direction of x and z respectively.

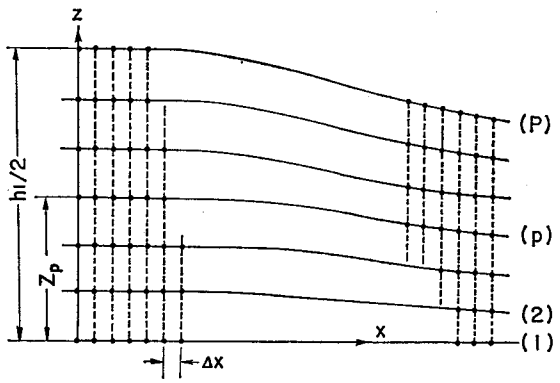

Fig. 1. Flow line model.

These values differ at each point in the deformation region. Because the material flow during flat rolling is laminar, each point on a flow line moves continuously along the same line. In the case of the material flow keeping volume constant as in a plastic deformation, the velocity components u and v are expressed by using the flow function $\psi(x, z)$ as follows:

$$u = \partial\psi/\partial z\,, \qquad v = -\partial\psi/\partial x\,. \tag{2}$$

From equation (1) and equation (2)

$$\psi(x, z) = \text{const.} \tag{3}$$

is obtained. Therefore, formula (3) shows the equation of the flow line. Equation (2) satisfies the following continuous equation(4) for the steady and two-dimensional flow.

$$\partial u/\partial x + \partial v/\partial z = 0\,. \tag{4}$$

Therefore, the value of the flow function can be regarded as the equivalence of the flow rate. Consequently, the line on the plate surface and the center line of the thickness in the direction of rolling are definitely regarded as the flow lines. From the fact that the value of the flow function on a flow line is always constant during the deformation, it is assumed that the value of the flow function $\psi(x, 0)$ on a flow line being equivalent to the center line of the thickness is zero. Now, the flow lines of the inner parts of the material are assumed to be solid lines, as shown in Fig. 1. Assuming that the distance from the center line ($\psi=0$) to a different optional flow line before the deformation is z_p, and that the entrance velocity of the material before the deformation into rolls is U_0, the value of the flow function on the flow line above mentioned is as follows:

$$\psi = U_0 \cdot z_p \tag{5}$$

This is always constant on the flow line from the start of deformation to the end. At the same time, assuming that the thickness of the plate before rolling is h_1, the value of the flow function ψ on the flow line of the surface is $U_0 \cdot h_1/2$. Generally, the strain rate components $\dot{\varepsilon}_x$, $\dot{\varepsilon}_z$ in the direction of x and z, and $\dot{\gamma}_{xz}$ on the xz-plane are expressed by the flow function $\psi(x, z)$ as follows:

$$\left.\begin{aligned} \dot{\varepsilon}_x &= \frac{\partial u}{\partial x} = \frac{\partial}{\partial x}\left(\frac{\partial \psi}{\partial z}\right) \\ \dot{\varepsilon}_z &= \frac{\partial v}{\partial z} = -\frac{\partial}{\partial z}\left(\frac{\partial \psi}{\partial x}\right) \\ \dot{\gamma}_{xz} &= \frac{\partial u}{\partial z} + \frac{\partial v}{\partial x} = \frac{\partial^2 \psi}{\partial z^2} - \frac{\partial^2 \psi}{\partial x^2} \end{aligned}\right\} \qquad (6)$$

2.2 Application of newly set lattice system for numerical calculation

Now, assuming that the P flow lines, as shown in Fig. 1, are determined by a rolling test, the distribution of the flow function values in the region of the deformation is known from the fact that the flow function values on these flow lines are always constant. Because the velocity components and the strain rate components are given in a form of the first and second partial differentiation of the flow function $\psi(x, z)$ with respect to x and z, the value of the flow function on the newly set each lattice point indicated in Fig. 2 must be known. The flow lines in the

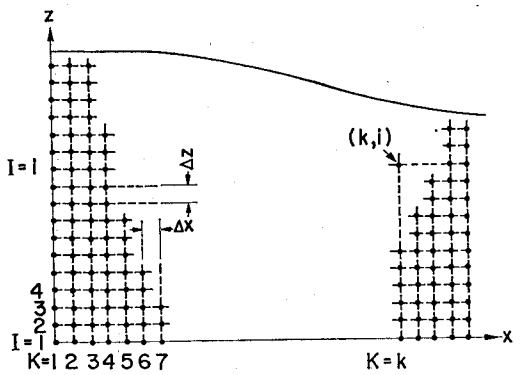

Fig. 2. The lattice model set up for the numerical calculation.

case of flat rolling are comparatively smooth. Therefore, even if these flow lines are given in a form of the polynomial, it is considered that no significant error is caused. For example, the equation of the p-th flow line, shown in Fig. 1, expressed by n-th order polynomial is:

$$z_p(x) = A_0^{(p)} + \sum_{j=1}^{n} A_j^{(p)} x^j \,, \tag{7}$$

where $A_j^{(p)}(j=0, 1, 2, \cdots, n)$ is constant, but which changes by each flow line. These constants can be pretty exactly calculated by the method of the least squares. It is known that the best value of n is 4-th order in the polynomial from the analytical results by computer. This will be seen in the case of the calculation example mentioned in the next section. Because each flow line is expressed by the corresponding polynomial as above mentioned, the value of the flow function on all flow lines in each lattice interval Δx in the x-direction is determined. Namely, the corresponding values of the flow function in the z-direction are obtained in accordance with the number of flow lines. Therefore, the value of the flow function at the optional point in the z-direction can be calculated by the interpolation method. Then, all values of the flow function at all lattice points shown in Fig. 2 can be obtained by the determination of the lattice interval Δz in the z-direction. As above mentioned, because the arrangement of the lattice points is parallel to the x- and z-axis, the velocity field and the strain rate field in all deformation region can be finite-differentially calculated from the values of the flow function at each lattice point.

2.3 Stress analysis

If the spreading in the width is regarded as negligible in flat rolling, the stress analysis can be performed as a plane strain deformation. The numerical calculation of the stress in material during rolling, shown in the next section, was made in accordance with the above condition, while the theoretical stress analysis, which is shown here, is discussed concerning three-dimensional deformation.

The rectangular co-ordinate systems i.e., x-, y- and z-axis are taken in the direction of rolling, material width and thickness. The equilibrium equation of three-dimensional deformation can be expressed by:

$$\left.\begin{aligned} \frac{\partial \sigma_x}{\partial x} + \frac{\partial \tau_{xy}}{\partial y} + \frac{\partial \tau_{zx}}{\partial z} &= 0 \\ \frac{\partial \tau_{xy}}{\partial x} + \frac{\partial \sigma_y}{\partial y} + \frac{\partial \tau_{yz}}{\partial z} &= 0 \\ \frac{\partial \tau_{zx}}{\partial x} + \frac{\partial \tau_{yz}}{\partial y} + \frac{\partial \sigma_z}{\partial z} &= 0 \,. \end{aligned}\right\} \tag{8}$$

Where σ_x, σ_y and σ_z are the normal stress components in the (x, y, z)-directions, and τ_{xy}, τ_{yz} and τ_{zx} are the shear stress components in the (x, y)-, (y, z)- and (x, z)-planes respectively.

The Levy-von Mises equations expressing the relation between the stress and strain rate for the plastic state of an isotropic material are as follows:

$$\left.\begin{aligned} \dot{\varepsilon}_x &= \frac{3}{2}\frac{\dot{\bar{\varepsilon}}}{\bar{\sigma}}(\sigma_x-\sigma_m), & \dot{\varepsilon}_y &= \frac{3}{2}\frac{\dot{\bar{\varepsilon}}}{\bar{\sigma}}(\sigma_y-\sigma_m), \\ \dot{\varepsilon}_z &= \frac{3}{2}\frac{\dot{\bar{\varepsilon}}}{\bar{\sigma}}(\sigma_z-\sigma_m), & \dot{\gamma}_{xy} &= 3\frac{\dot{\bar{\varepsilon}}}{\bar{\sigma}}\tau_{xy}, \\ \dot{\gamma}_{yz} &= 3\frac{\dot{\bar{\varepsilon}}}{\bar{\sigma}}\tau_{yz}, & \dot{\gamma}_{zx} &= 3\frac{\dot{\bar{\varepsilon}}}{\bar{\sigma}}\tau_{zx} \end{aligned}\right\} \tag{9}$$

where $\dot{\varepsilon}_x$, $\dot{\varepsilon}_y$ and $\dot{\varepsilon}_z$ are the normal strain rate components in the (x, y, z)-directions, and $\dot{\gamma}_{xy}$, $\dot{\gamma}_{yz}$ and $\dot{\gamma}_{zx}$ are the shear strain rate components in the (x, y)-, (y, z)- and (z, x)-planes respectively. Also:

$$\left.\begin{aligned} \sigma_m &= (\sigma_x+\sigma_y+\sigma_z)/3 \\ \bar{\sigma} &= \{(\sigma_x-\sigma_y)^2+(\sigma_y-\sigma_z)^2+(\sigma_z-\sigma_x)^2+6(\tau_{xy}^2+\tau_{yz}^2+\tau_{zx}^2)\}^{1/2}/\sqrt{2} \\ \dot{\bar{\varepsilon}} &= \sqrt{2}\{(\dot{\varepsilon}_x-\dot{\varepsilon}_y)^2+(\dot{\varepsilon}_y-\dot{\varepsilon}_y)^2+(\dot{\varepsilon}_z-\dot{\varepsilon}_x)^2+3(\dot{\gamma}_{xy}^2+\dot{\gamma}_{yz}^2+\dot{\gamma}_{zx}^2)/2\}^{1/2}/3. \end{aligned}\right\} \tag{10}$$

The following equation is obtained from Eq. (9)

$$\sigma_x = \sigma_y+\frac{2}{3}\frac{\bar{\sigma}}{\dot{\bar{\varepsilon}}}(\dot{\varepsilon}_x-\dot{\varepsilon}_y). \tag{11}$$

By introducing Eq. (8) after partially differentiating boths sides of Eq. (11) by y:

$$\frac{\partial\sigma_x}{\partial y} = \frac{2}{3}\frac{\partial}{\partial y}\left\{\frac{\bar{\sigma}}{\dot{\bar{\varepsilon}}}(\dot{\varepsilon}_x-\dot{\varepsilon}_y)\right\}-\left(\frac{\partial\tau_{xy}}{\partial x}+\frac{\partial\tau_{yz}}{\partial z}\right). \tag{12}$$

Moreover, integrating Eq. (12) by y after substituting the terms of shear strain rate components $\dot{\gamma}_{xy}$ and $\dot{\gamma}_{yz}$ in place of τ_{xy} and τ_{yz}:

$$\sigma_x = \int_{y_0}^{y}\left[\frac{2}{3}\frac{\partial}{\partial y}\left\{\frac{\bar{\sigma}}{\dot{\bar{\varepsilon}}}(\dot{\varepsilon}_x-\dot{\varepsilon}_y)\right\}-\frac{1}{3}\frac{\partial}{\partial x}\left(\frac{\bar{\sigma}}{\dot{\bar{\varepsilon}}}\dot{\gamma}_{xy}\right)-\frac{1}{3}\frac{\partial}{\partial z}\left(\frac{\bar{\sigma}}{\dot{\bar{\varepsilon}}}\dot{\gamma}_{yz}\right)\right]dy+F(x, z), \tag{13}$$

where $F(x, z)$ is the integrating constant and the function of x and z. $F(x, z)$ satisfies the following relation:

$$\sigma_x|_{y=y_0} = F(x, z), \tag{14}$$

and

$$\left.\frac{\partial\sigma_x}{\partial x}\right|_{y=y_0} = -\frac{1}{3}\left[\frac{\partial}{\partial y}\left(\frac{\bar{\sigma}}{\dot{\bar{\varepsilon}}}\dot{\gamma}_{xy}\right)+\frac{\partial}{\partial z}\left(\frac{\bar{\sigma}}{\dot{\bar{\varepsilon}}}\dot{\gamma}_{zx}\right)\right]_{y=y_0} = \frac{\partial}{\partial x}F(x, z) \tag{15}$$

is obtained. Consequently, $F(x, z)$ is shown as follows:

$$F(x, z) = -\frac{1}{3}\int_{x_0}^{x}\left[\frac{\partial}{\partial y}\left(\frac{\bar{\sigma}}{\dot{\bar{\varepsilon}}}\dot{\gamma}_{xy}\right)+\frac{\partial}{\partial z}\left(\frac{\bar{\sigma}}{\dot{\bar{\varepsilon}}}\dot{\gamma}_{zx}\right)\right]_{y=y_0}dx+\sigma_1(z) \tag{16}$$

Where $\sigma_1(z)$ is the integrating constant. From Eq. (13), the relation between σ_x and $F(x, z)$ can be expressed by the following form:

$$\left.\frac{\partial \sigma_x}{\partial z}\right|_{y=y_0} = \frac{\partial}{\partial z}F(x, z)\,. \tag{17}$$

Moreover, σ_x can also be expressed by using the following equation

$$\sigma_x = \sigma_z + \frac{2}{3}\frac{\bar{\sigma}}{\dot{\bar{\varepsilon}}}(\dot{\varepsilon}_x - \dot{\varepsilon}_z)\,. \tag{18}$$

Consequently, the following equation i.e.,

$$\begin{aligned}\frac{\partial \sigma_x}{\partial z} &= \frac{\partial \sigma_z}{\partial z} + \frac{2}{3}\frac{\partial}{\partial z}\left\{\frac{\bar{\sigma}}{\dot{\bar{\varepsilon}}}(\dot{\varepsilon}_x - \dot{\varepsilon}_z)\right\} \\ &= \frac{2}{3}\frac{\partial}{\partial z}\left\{\frac{\bar{\sigma}}{\dot{\bar{\varepsilon}}}(\dot{\varepsilon}_x - \dot{\varepsilon}_z)\right\} - \frac{1}{3}\frac{\partial}{\partial x}\left(\frac{\bar{\sigma}}{\dot{\bar{\varepsilon}}}\dot{\gamma}_{zx}\right) - \frac{1}{3}\frac{\partial}{\partial y}\left(\frac{\bar{\sigma}}{\dot{\bar{\varepsilon}}}\dot{\gamma}_{yz}\right)\end{aligned} \tag{19}$$

is obtained from Eq. (8) and Eq. (9). Using Eq. (17),

$$\frac{\partial}{\partial z}F(x, z) = \left[\frac{2}{3}\frac{\partial}{\partial z}\left\{\frac{\bar{\sigma}}{\dot{\bar{\varepsilon}}}(\dot{\varepsilon}_x - \dot{\varepsilon}_z)\right\} - \frac{1}{3}\frac{\partial}{\partial x}\left(\frac{\bar{\sigma}}{\dot{\bar{\varepsilon}}}\dot{\gamma}_{zx}\right) - \frac{1}{3}\frac{\partial}{\partial y}\left(\frac{\bar{\sigma}}{\dot{\bar{\varepsilon}}}\dot{\gamma}_{yz}\right)\right]_{y=y_0} \tag{20}$$

Therefore, $F(x, z)$ can be presented by integrating both sides of Eq. (20) by z as follows:

$$F(x, z) = \int_{z_0}^{z}\left[\frac{2}{3}\frac{\partial}{\partial z}\left\{\frac{\bar{\sigma}}{\dot{\bar{\varepsilon}}}(\dot{\varepsilon}_x - \dot{\varepsilon}_z)\right\} - \frac{1}{3}\frac{\partial}{\partial x}\left(\frac{\bar{\sigma}}{\dot{\bar{\varepsilon}}}\dot{\gamma}_{zx}\right) - \frac{1}{3}\frac{\partial}{\partial y}\left(\frac{\bar{\sigma}}{\dot{\bar{\varepsilon}}}\dot{\gamma}_{yz}\right)\right]_{y=y_0} dz + \sigma_2(x)\,, \tag{21}$$

where $\sigma_2(x)$ is the integrating constant and satisfies the next relation.

$$\sigma_2(x) = F(x, z)\,|_{z=z_0} = F(x, z_0)\,. \tag{22}$$

Then, $F(x, z_0)$ is expressed using Eq. (16) as in the following form. Namely,

$$F(x, z_0) = -\int_{x_0}^{x}\frac{1}{3}\left[\frac{\partial}{\partial y}\left(\frac{\bar{\sigma}}{\dot{\bar{\varepsilon}}}\dot{\gamma}_{xy}\right) + \frac{\partial}{\partial z}\left(\frac{\bar{\sigma}}{\dot{\bar{\varepsilon}}}\dot{\gamma}_{zx}\right)\right]_{y=y_0, z=z_0} dx + \sigma_1(z_0) \tag{23}$$

Now, setting $\sigma_1(z_0) = \sigma_0$, $\sigma_2(x)$ is shown from Eq. (22) as follows:

$$\sigma_2(x) = -\int_{x_0}^{x}\frac{1}{3}\left[\frac{\partial}{\partial y}\left(\frac{\bar{\sigma}}{\dot{\bar{\varepsilon}}}\dot{\gamma}_{xy}\right) + \frac{\partial}{\partial z}\left(\frac{\bar{\sigma}}{\dot{\bar{\varepsilon}}}\dot{\gamma}_{zx}\right)\right]_{y=y_0, z=z_0} dx + \sigma_0 \tag{24}$$

Therefore, $F(x, z)$ can be determined from Eq. (21) as follows:

$$\begin{aligned}F(x, z) = &\int_{z_0}^{z}\left[\frac{2}{3}\frac{\partial}{\partial z}\left\{\frac{\bar{\sigma}}{\dot{\bar{\varepsilon}}}(\dot{\varepsilon}_x - \dot{\varepsilon}_z)\right\} - \frac{1}{3}\frac{\partial}{\partial x}\left(\frac{\bar{\sigma}}{\dot{\bar{\varepsilon}}}\dot{\gamma}_{zx}\right)\right] - \frac{1}{3}\frac{\partial}{\partial y}\left(\frac{\bar{\sigma}}{\dot{\bar{\varepsilon}}}\dot{\gamma}_{yz}\right)\Big]_{y=y_0} dz \\ &- \int_{x_0}^{x}\frac{1}{3}\left[\frac{\partial}{\partial y}\left(\frac{\bar{\sigma}}{\dot{\bar{\varepsilon}}}\dot{\gamma}_{xy}\right) + \frac{\partial}{\partial z}\left(\frac{\bar{\sigma}}{\dot{\bar{\varepsilon}}}\dot{\gamma}_{zx}\right)\right]_{y=y_0, z=z_0} dx + \sigma_0\,.\end{aligned} \tag{25}$$

Finally, σ_x can be expressed substituting this function $F(x, z)$ into Eq. (13), as shown in the following formula. i.e.,

$$\begin{aligned}\sigma_x = &\int_{y_0}^{y}\left[\frac{2}{3}\frac{\partial}{\partial y}\left\{\frac{\bar{\sigma}}{\dot{\bar{\varepsilon}}}(\dot{\varepsilon}_x-\dot{\varepsilon}_y)\right\}-\frac{1}{3}\frac{\partial}{\partial x}\left(\frac{\bar{\sigma}}{\dot{\bar{\varepsilon}}}\dot{\gamma}_{xy}\right)-\frac{1}{3}\frac{\partial}{\partial z}\left(\frac{\bar{\sigma}}{\dot{\bar{\varepsilon}}}\dot{\gamma}_{yz}\right)\right]dy\\ &+\int_{z_0}^{z}\left[\frac{2}{3}\frac{\partial}{\partial z}\left\{\frac{\bar{\sigma}}{\dot{\bar{\varepsilon}}}(\dot{\varepsilon}_x-\dot{\varepsilon}_z)\right\}-\frac{1}{3}\frac{\partial}{\partial x}\left(\frac{\bar{\sigma}}{\dot{\bar{\varepsilon}}}\dot{\gamma}_{zx}\right)-\frac{1}{3}\frac{\partial}{\partial y}\left(\frac{\bar{\sigma}}{\dot{\bar{\varepsilon}}}\dot{\gamma}_{yz}\right)\right]_{y=y_0}dz\\ &-\int_{x_0}^{x}\frac{1}{3}\frac{\partial}{\partial y}\left(\frac{\bar{\sigma}}{\dot{\bar{\varepsilon}}}\dot{\gamma}_{xy}\right)+\frac{\partial}{\partial z}\left(\frac{\bar{\sigma}}{\dot{\bar{\varepsilon}}}\dot{\gamma}_{zx}\right)\Big]_{y=y_0,\ z=z_0}dx+\sigma_0\,,\end{aligned}\tag{26}$$

where σ_0 is evidently the stress in the x-direction at the origin of the co-ordinate axis (x_0, y_0, z_0) from the analytical process of Eq. (6). σ_x being determined, all stress components are obtained from Eq. (9)

If the spreading in the width is regarded as negligible in flat rolling, the mechanics of plane strain plastic deformation can be applied. In this case,

$$\dot{\varepsilon}_y=\dot{\gamma}_{xy}=\dot{\gamma}_{yz}=0\,.\tag{27}$$

At the same time, the terms of the partial differentiation by y included in Eq. (26) are all zero, and then σ_x is simplified as follows:

$$\sigma_x=\int_{x_0}^{x}\left[\frac{2}{3}\frac{\partial}{\partial z}\left\{\frac{\bar{\sigma}}{\dot{\bar{\varepsilon}}}(\dot{\varepsilon}_x-\dot{\varepsilon}_z)\right\}-\frac{1}{3}\frac{\partial}{\partial x}\left(\frac{\bar{\sigma}}{\dot{\bar{\varepsilon}}}\dot{\gamma}_{zx}\right)\right]dz-\int_{x_0}^{x}\left[\frac{1}{3}\frac{\partial}{\partial z}\left(\frac{\bar{\sigma}}{\dot{\bar{\varepsilon}}}\dot{\gamma}_{zx}\right)\right]_{z=z_0}dx+\sigma_0\,,\tag{28}$$

the material is rolled without front and back tension, then $\sigma_0=0$. The deformation of the material element on the center level ($z=0$) in the thickness is only the elongation without a slip flow. Namely,

$$\dot{\gamma}_{zx}|_{z=0}=0\,.\tag{29}$$

Therefore, Eq. (28) can be more simplified as follows:

$$\sigma_x=\int_0^{z}\left[\frac{2}{3}\frac{\partial}{\partial z}\left\{\frac{\bar{\sigma}}{\dot{\bar{\varepsilon}}}(\dot{\varepsilon}_x-\dot{\varepsilon}_z)\right\}-\frac{1}{3}\frac{\partial}{\partial x}\left(\frac{\bar{\sigma}}{\dot{\bar{\varepsilon}}}\dot{\gamma}_{zx}\right)\right]dz\,.\tag{30}$$

In this case, the effective stress $\bar{\sigma}$ and the effective strain rate $\dot{\bar{\varepsilon}}$ are defined by

$$\left.\begin{aligned}\bar{\sigma}&=\{3(\sigma_x-\sigma_z)^2/4+3\tau_{xz}^2\}^{1/2}\\ \dot{\bar{\varepsilon}}&=2(3\dot{\varepsilon}_x^2+3\dot{\gamma}_{zx}^2/4)^{1/2}/3\end{aligned}\right\}\tag{31}$$

If the effective stress $\bar{\sigma}$ is only a known function of the effective finite strain, $\bar{\varepsilon}$ must be obtained along the actual flow path of each particle by integration, i.e.,

$$\bar{\varepsilon}=\int_0^{t}\dot{\bar{\varepsilon}}dt\,,\tag{32}$$

where t is the necessary time, which is measured from the starting point of the deformation.

III. Calculated example concerning strain rate components and stress components in material during rolling

3.1 Rolling test for the determination of the flow lines

The rolled material used for this test was the commercial 2S-Aluminium plate with $h_1=25$ (mm) in thickness and $b'=59.5$ (mm) in width. Two pieces of Al-plates were fastened in the width direction with two bolts, at the top and bottom. On consideration, the total width $b=2b'=119$ (mm) as shown in Fig. 3(a). On the contact sides, the circles of 2 (mm) in diameter are drawn by etching

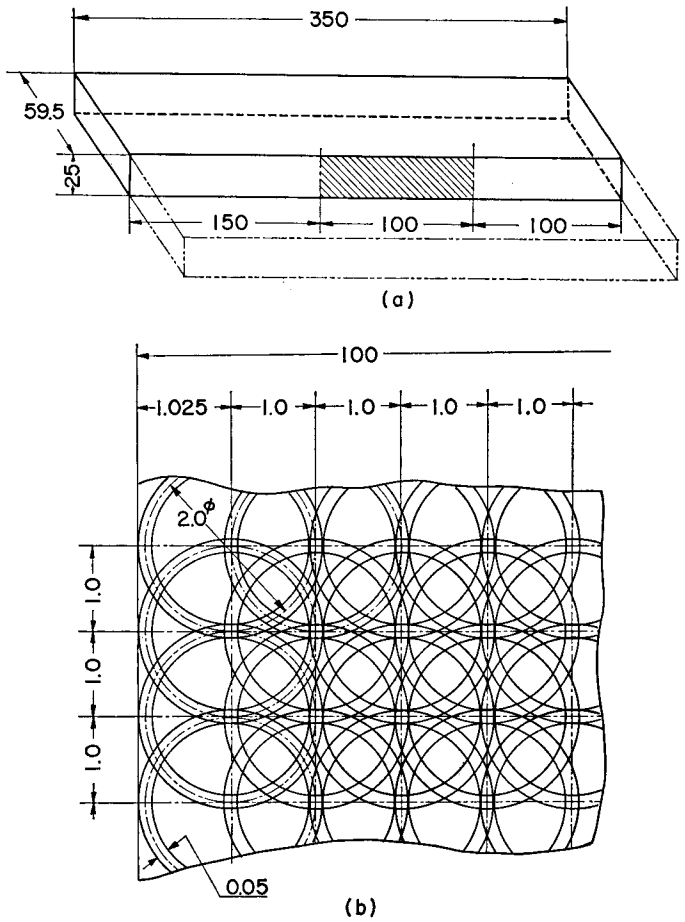

Fig. 3. Dimension of the material used for the rolling tests (a) and the shape of pattern made by etching on the side (b).

the center at each lattice point with the interval of 1 (mm), as shown in Fig. 3(b). The relationship between the stress and strain of the Aluminium used in this experiment was obtained by the compression test as shown in Fig. 4, and formulated as follows:

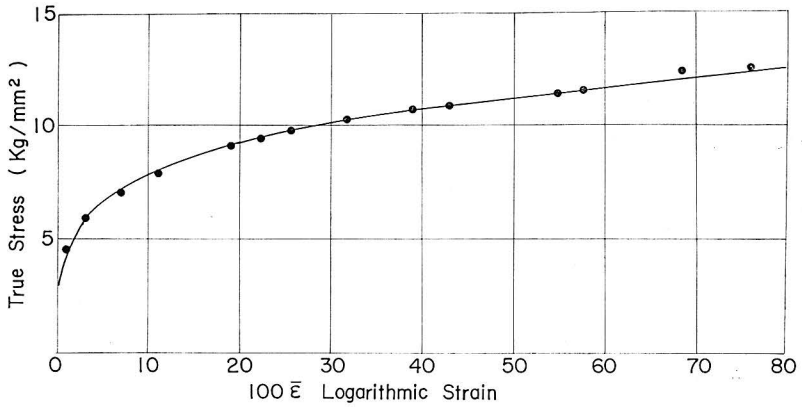

Fig. 4. Relationship between stress and strain of aluminium used in this experiment.

$$\bar{\sigma} = 13.1\bar{\varepsilon}^{0.22}, \tag{33}$$

where $\bar{\sigma}$ and $\bar{\varepsilon}$ are the effective stress and the effective strain. This material was rolled from $h_1=25$ (mm) to $h_2=17$ (mm) with the entrance velocity $U_0=22.6$ (mm/s) into work rolls of 180 (mm) in diameter and with back-up rolls of 350 (mm). This rolling test was performed under a cold and non-lubricant condition. Fig. 5 shows a deformation example of the pattern obtained from the rolling test. In general, the flow line can be obtained by jointing the corresponding intersection

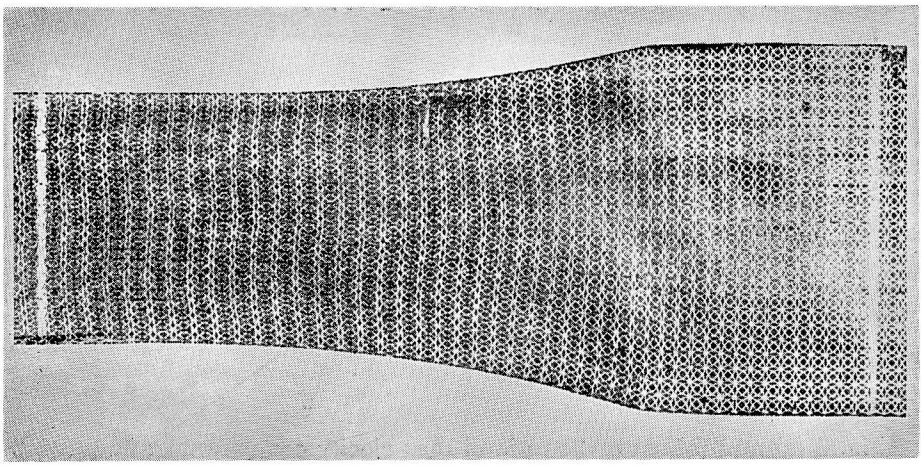

Fig. 5. Deformation example of the pattern obtained from the rolling test.

of two circles adjoining each other. One circle has 12 intersected points with other circles. Among them, 2 of 10 points place on the same flow line. Because the etching made on the designated plate side is technically difficult, the positions of the lattice points for several test pieces may not be necessarily exact. However, 12 circles in the z- direction are obtained in half thickness of the plate and 12 flow lines are determined by, for example, jointing the center points of each deformed circle along the actual flow path of each particle. Approximating the vertical distance z from the center line of the test plate to each flow line obtained from each test piece by 4-th order equations of x in the rolling direction, and connecting continuously the corresponding points which are divided into 13 equal parts from $F=1$ (Center line) to $F=14$ (Flow line of plate surface) using a least square method, the flow lines as shown in the solid lines of Fig. 6 can be obtained. For the numerical calculation of the velocity components, the strain rate components and the stress components in the rolled material, the lattice points in parallel to x- and z-axis are to be established, as shown in Fig. 2. The dotted lines in Fig. 6 show that the calculation interval in the deformation zone in the

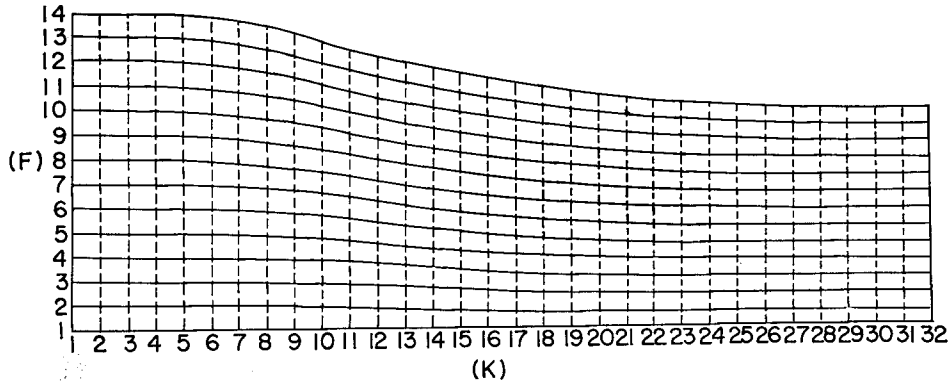

Fig. 6. Flow lines obtained from the rolling test (solid line).

material is divided into 31 equal parts of $\Delta x=1.118$ (mm) in the rolling direction i.e., from $K=1$ to $K=32$ in terms of the lattice point number. On the other hand, the half thickness of the plate is divided into equal parts of $\Delta z=0.568$ (mm), and $I=1$ is set on the center of the plate thickness. The number of the lattice points in the non-deformed zone is established from $I=1$ to $I=23$ in parallel to the z-axis.

3.2 Calculated results

Fig. 7 (a) and (b) show the ratio of the velocity components u and v in the rolling direction and in the thickness direction, respectively, to the moving velocity

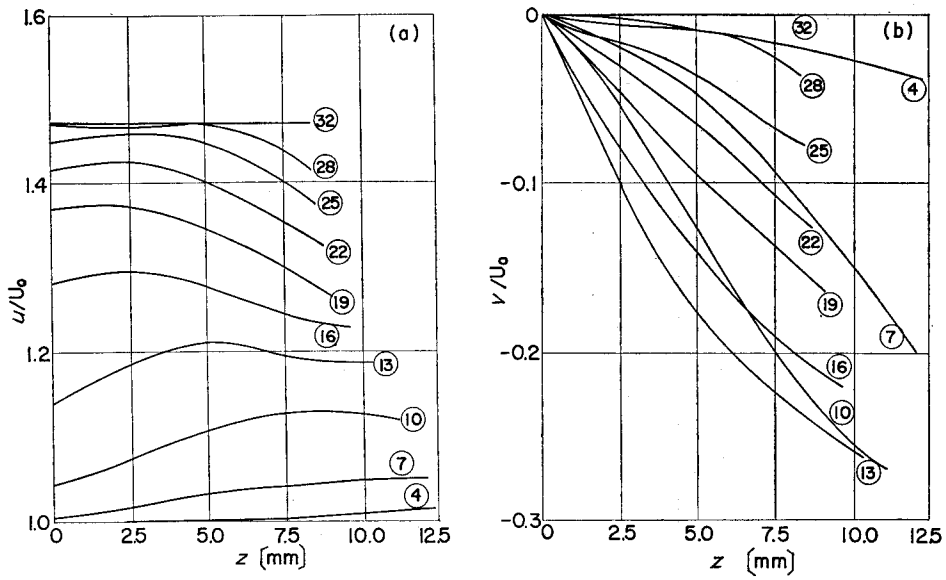

Fig. 7. Velocity component u in the rolling direction of the plate (a) and v in the thickness direction (b).

U_0 of the material toward the rolls. The abscissa takes the distance measured in the z-direction from the center of the plate thickness. The integers in the circles indicated in these figures express the number K of the lattice points in the

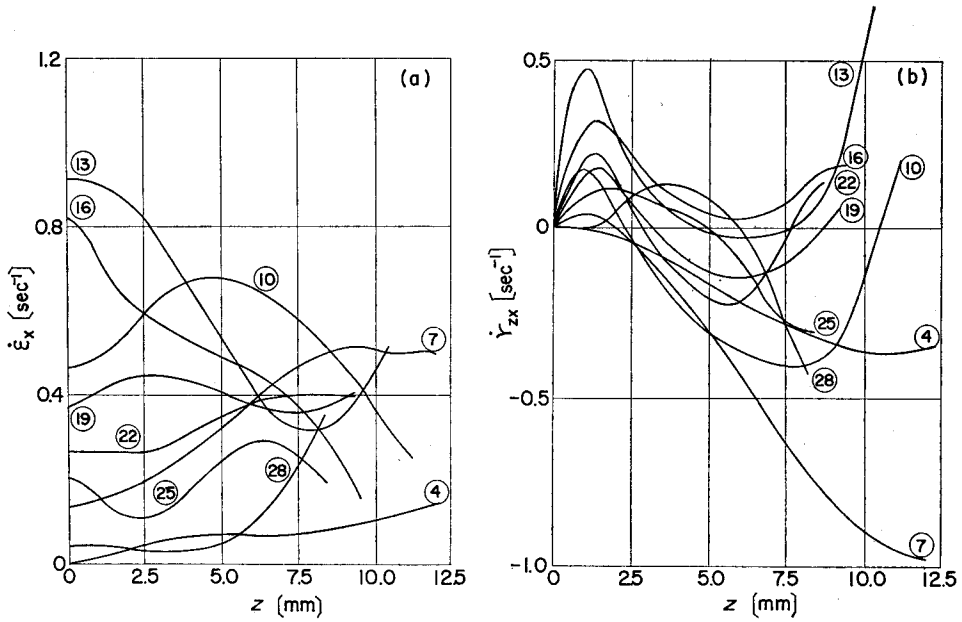

Fig. 8. Strain rate $\dot{\varepsilon}_x$ in the rolling direction (a) and shearing strain rate $\dot{\gamma}_{zx}$ (b).

x-direction.

Fig. 8 (a) and (b) show the distribution of the strain rate components $\dot{\varepsilon}_x$ $(=-\dot{\varepsilon}_z)$ in the rolling direction and that of the shear strain rate components $\dot{\gamma}_{zx}$.

Fig. 9 shows the distribution of the effective strain. Because the deforma-

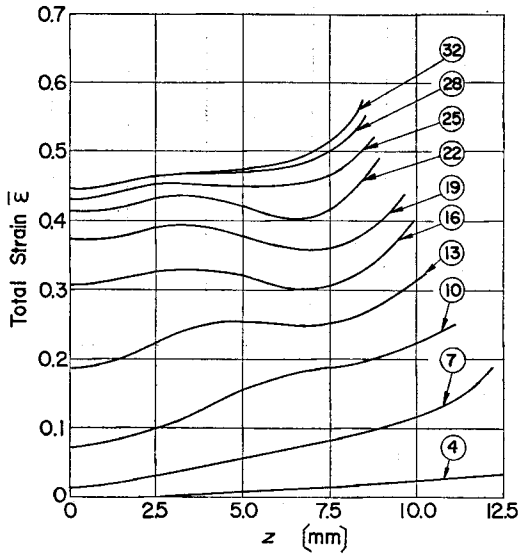

Fig. 9. Distribution of equivalent strain in material.

tion on the center line of the plate thickness does not cause any slipping, the effective incremental strain $d\bar{\varepsilon}$ is equal to $1.15 \cdot \varepsilon_z$ in plane strain deformation. Consequently, the effective strain $\bar{\varepsilon}=1.15 \ln(h_1/h_2)=0.444$ at the end point of the deformation because of the actual flow path in one way. This value coincides with that on the center line at the lattice point number $K=32$ (at the end point of the deformation).

Fig. 10 (a) and (b) show the distribution of the stress components σ_x and σ_z respectively on each flow line, where F indicates the number of flow lines. The curve of $F=14$ in these figures is the distribution of stress on the plate surface. The stress σ_x in the rolling direction is the compression in the beginning zone of the deformation, the tension in the central zone and the compression once more in the finishing zone, as shown in Fig. 10 (a). The stress σ_z in the thickness direction has a maximum value in the finishing zone of the deformation, and a minimum value in the central zone of the deformation. This influence is more conspicuous near the plate surface.

Fig. 11 (a) and (b) show the distribution of the stress σ_s in the direction of the flow line and that of the stress σ_n in the normal direction for the flow line.

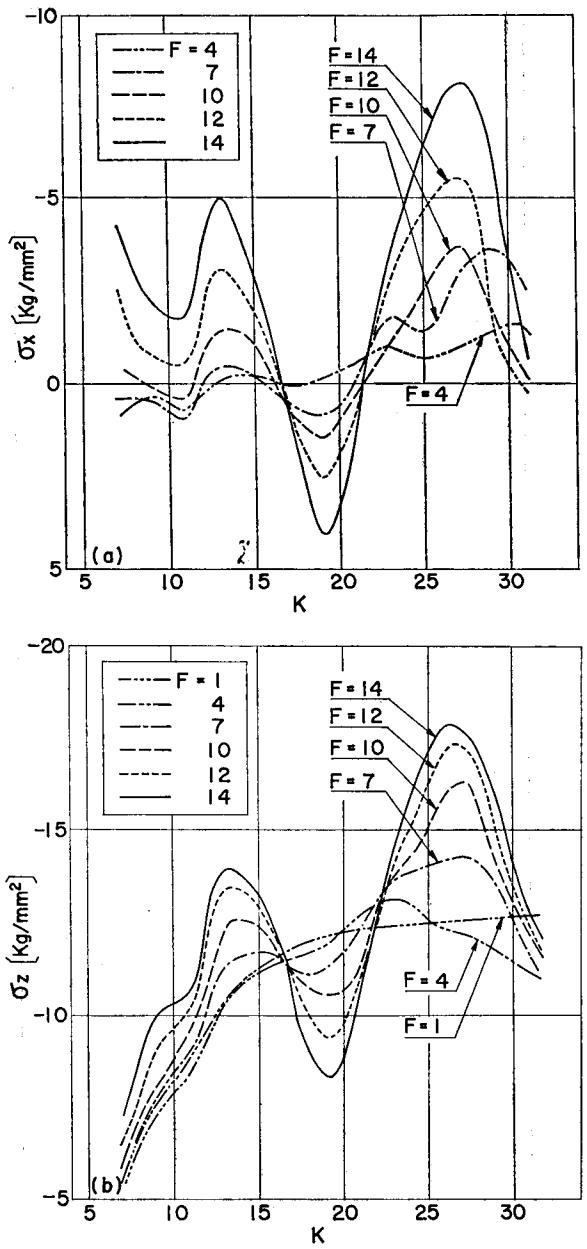

Fig. 10. Stress component σ_x in the rolling direction on each flow line (a) and σ_z in the thickness direction (b).

The curve of $F=14$ in Fig. 11 (b) shows the distribution of σ_n on the plate surface, and is regarded as that of the roll pressure. This distribution of the roll pressure has a comparably remarkable concave zone in the center of the contact

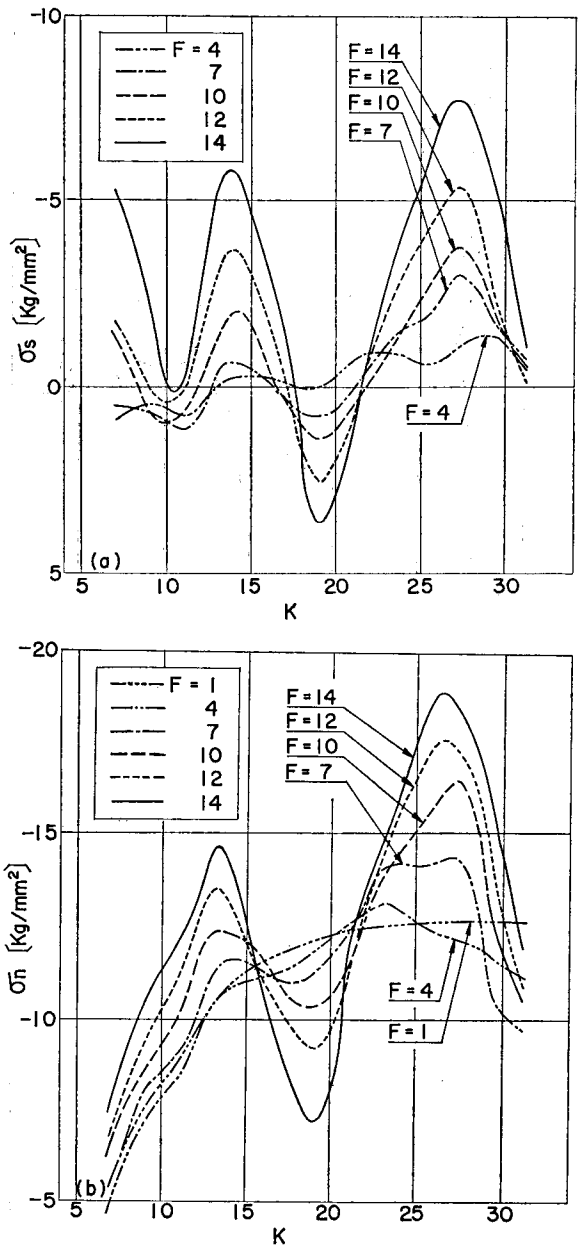

Fig. 11. Distribution of stress component in the tangential direction of each flow line (a) and σ_n in the normal direction (b).

surface between the rolls and the plate.

Fig. 12 shows the distribution of the shearing stress τ_{ns} on the flow line. The position where the value of τ_{ns} on the plate surface varies from plus to minus

near the end zone of deformation is regarded as a neutral point. The gradient of the shearing stress at this point is remarkably acute.

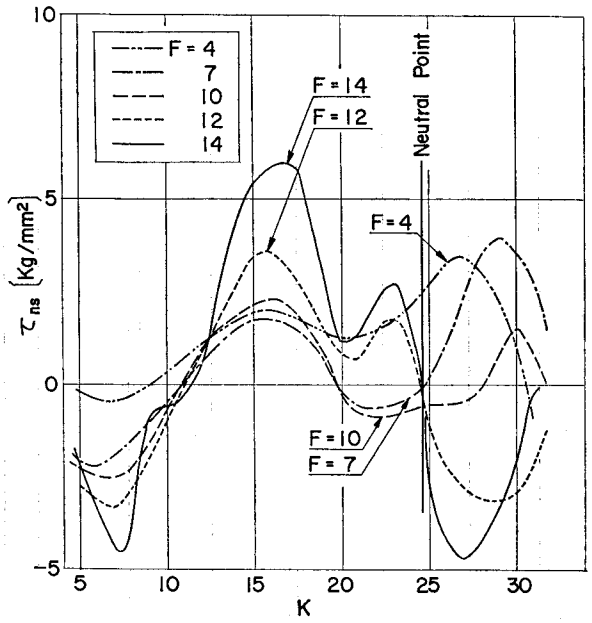

Fig. 12. Shearing stress τ_{ns} on each flow line.

3.3 Examinations for the calculated results

The accuracy of the calculated results by the visioplasticity method depends absolutely on that of the rolling test for determining the flow lines, because the manner in which the solution is derived is a result of a combination of experience and theory. The fact is that the correct estimate for the calculated values concerning the stress cannot be examined in detail because of the default of the examples of the experimentally measured values of the stress in the material. Each distribution of the stress components calculated on the flow lines takes the form of a comparably acute rise and fall on the whole. In particular, the distribution of σ_z in the thickness direction on the plate surface has a remarkable concave zone in the center part of the deformation. This differs largely from the form of the friction hill obtained by Karman's rolling equation. It may be that the elastic stress components of Al-plates used for the test pieces are not taken into account.

The rolling force was measured by a load cell during rolling, when rolling tests for determining the flow lines were performed. The result was that the rolling force was 37.7 (ton). On the other hand, the rolling force calculated from the distribution of σ_z in the thickness direction on the contact surface between

the rolls and the Al-plate was 38.6 (ton). This calculated value agrees comparably well with the measured value. As shown in Fig. 12, the position of the neutral point obtained from the distribution of the shearing stress on the contact surface is regarded as generally valid. Fig. 13 shows the resultant velocity in the direc-

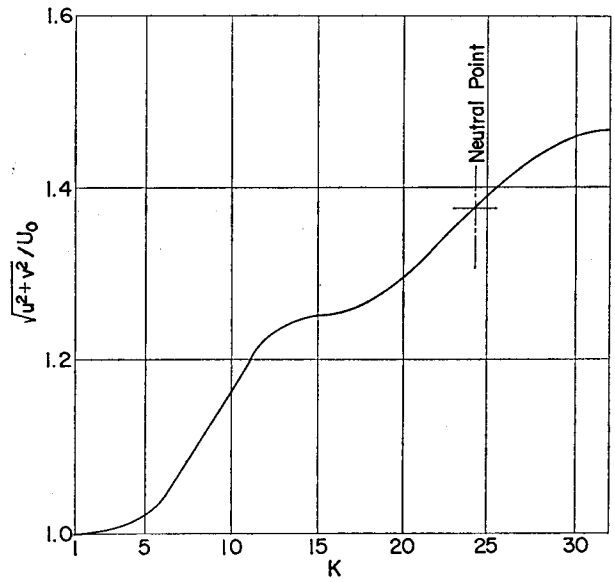

Fig. 13. Velocity distribution on the surface of plate.

tion of the flow line on the plate surface, which is obtained from Fig. 7 (a) and (b). The ratio of the forward slip is 1.067 in this case, and this value is not so unreasonable. The value of the resultant velocity increases gradually in the rolling direction, which results in a sliding friction on the whole contact surface. The idea of the sticking friction on the whole contact surface, which is represented by Sims' rolling theory, is dominant in the case of the hot rolling of steel without lubrication. However, this idea leaves room for further investigation.

IV. Conclusion

The visioplasticity analysis on stress in block during rolling is discussed and then the calculable results of the stress concerning the inside and surface of block are presented in the case where the Al-plate with a thickness of 25 mm is rolled to 17 mm. This stress analysis depends considerably on the accuracy of the rolling test, which is carried out in order to determine the flow line. It is very difficult to deduce the validity of the calculable results in detail because of the lack of measured examples on the stress in block. In particular, the distribution of the surface

stress in the thickness direction is remarkably concaved in the central part of the deformation region. Also, it is different from the shape of the friction hill, which is obtained by solving Karman's rolling equation.

The measured roll force by a load cell coincides extremely well with that obtained from the stress in the thickness direction which is calculated here. The neutral point seems to exist on the valid position. Of course, the validity of the calculated results may not be concluded from only the two points mentioned above. However, it may be possible to apply the visioplasticity method for the calculation of the stress in block, if the exact flow can be determined.

References

1) Karman, Th.: Z. angew. Math. Mechan., 5(1925), p. 139.
2) Trinks, W.: Blast Furn. Steel Pl., 25(1937), p. 135.
3) Nadai, A.: J. Appl. Mechan., 1937, p. 54.
4) Orowan, E.: Proc. Inst. Mech. Eng., 150(1943), p. 140.
5) Sims, R.B.: J. Iron Steel Inst., 168(1951), p. 57.
6) Siebel, E. und Lueg, W.: Kaiser-Wilhelm-Inst. Eisenforsch. Duesseldorf. 15, 1–14(1933).
7) Y. Matsuura, M. Motomura, T. Omiya and K. Kato: Sosei to Kako (J. JSTP), **13**, 138 (1972), p. 481.
8) S. Teshima and M. Koga: ibid., **16**, 179(1975), p. 1124.
9) E.G. Thomsen and J.T. Lapsley, Jr.: Proc. Soc. Exp. Stress Anal., **11**, 2(1954), p. 59.
10) A. Shabaik and S. Kobayashi: Trans. ASME., May 1967, p. 339.
11) A. Shabaik and E.G. Thomsen: ibid., Aug. 1969, p. 543.
12) A. Shabaik, S. Kobayashi and E.G. Thomsen: ibid., Aug. 1967, p. 503.
13) H. Ishikawa, K. Kato and M. Goto: Sosei to Kako (J. JSTP), **16**, 169(1975), p. 140.